ELSEVIER

Journal of Nuclear Materials 250 (1997) 96–102

journal of nuclear materials

A collisional–radiative cooling model for light impurity elements in hot plasmas under non-equilibrium conditions

G. Veres [a], L.L. Lengyel [b,*]

[a] *KFKI-Research Institute for Particle and Nuclear Physics, PoB 49, H-1525 Budapest, Hungary*
[b] *Max-Planck-Institut für Plasmaphysik, EURATOM Association, D-85748 Garching, Germany*

Received 12 February 1997; accepted 9 September 1997

Abstract

The power radiated by low-temperature high-density impurity inclusions in plasmas, such as the clouds surrounding ablating impurity pellets, or the vapor layers evolving over vaporizing surfaces subjected to high-temperature plasmas, is calculated by means of a collisional–radiative (CR) model without the usual assumptions of equilibrium conditions. The populations of the ionization levels are determined by finite-rate calculations and, due to the much shorter characteristic times involved, instantaneous relaxation is assumed for the intermediate excitation levels considered. Data obtained with this model in the low-density limit are compared with those of Post–Jensen corona model [D.E. Post, R.V. Jensen et al., At. Data and Nucl. Data Tables 20 (1977) 397; R. Clark, J. Abdallah, D.E. Post, J. Nucl. Mater. 220–222 (1995) 1028; D.E. Post, J. Nucl. Mater. 220–222 (1995) 143]. Results of representative scenario calculations pertaining to the ablation of carbon and neon pellets are presented. © 1997 Elsevier Science B.V.

PACS: 52.25.Vy; 52.55.Dy; 52.65.− y

1. Introduction

The radiation power emitted by low-temperature high-density impurity inclusions in magnetically confined high-temperature plasmas is of current practical interest. Impurity pellets are being injected into magnetically confined fusion plasmas prior to disruptions for mitigating the process by fast radiative cooling thus reducing the thermal and electro-mechanical loads affecting the structure [4,5]. In the case of plasma–wall contact, intense vaporization may set in and last until a protective vapor layer evolves at the solid surface. The thermodynamic and shielding characteristics of this layer depend upon the magnitude of the radiation losses exiting the partially or fully ionized vapor. In both cases mentioned, an accurate determination of the radiation losses is of primary interest. Since the processes considered involve, besides atomic and plasma physics, hydrodynamic and MHD phenomena, the respective time scales may be vastly different from those of radiative processes. Therefore, in the majority of calculations pertaining to such processes, the losses were usually calculated on the basis of simplifying assumptions such as corona equilibrium conditions, or like. For the case of corona equilibrium, the Post–Jensen model [1–3] offers a convenient and fast computational way for estimating the radiation losses. However, the vapor clouds evolving at vaporizing or ablating surfaces are usually high-density low-temperature partially ionized gases far away from corona equilibrium conditions.

The objective of the present work is to provide a radiation model that is accurate enough for predictive calculations yet simple enough to avoid excessive computational times. Note that in up-to-date hydrodynamic and MHD models treating surface vaporization and pellet abla-

* Corresponding author. Tel.: +49-89 3299 1626; fax: +49-89 3299 2580; e-mail: lll@ipp-garching.mpg.de.

PII S0022-3115(97)00295-X

tion phenomena ionization and recombination are calculated by means of finite rates, without assuming equilibrium conditions. This fact offers a convenient way for combining two codes and to compute simultaneously the radiation losses inherent in these processes without the usual corona equilibrium or LTE (local thermal equilibrium) assumptions. In its extent, the present model is similar to the Post–Jensen model [1,2], or to its updated version [3], but is applicable also to the low-temperature high-density plasma domain under non-equilibrium conditions. A more elaborate radiation model was developed by Behringer some time ago [6]. However, the computational requirements (computer time) associated with this model pose some difficulties when applied to hydrodynamic calculations in which radiation is only a part of the physical processes that must be followed up simultaneously. The model described here is to bridge the gap between the Post–Jensen model and more elaborate models used for non-equilibrium radiation calculations.

With the help of the present model, the radiated power can be calculated at any electron density value starting from the corona limit up to the LTE limit. This is made possible by the proper selection of the various transitions to be included into the rate equations. For each element, only a limited number of transitions are considered. It is made certain that the rest, which is neglected, does not cause an error larger than a few percent of the radiative power emitted.

The method is applicable primarily to light elements in which case the number of relevant transitions and excited levels is within reasonable limits. Difficulties arise if one tries to extend the method to cover heavy elements because of the limited availability of data on transition probabilities and the excessive computational procedures required in this case.

Throughout the present analysis, the following notation shall be used: n_e and T_e, electron density and temperature, n, population densities of the excited levels, N, ion densities, z, ionic charge (Z-number), p and q, excited levels, g, the ground states of the neutrals and ions considered, k, Boltzmann constant. Unless otherwise indicated, the SI (mks) system of units is used.

2. The model

Impurities in plasmas can mainly radiate power due to three different atomic-physical processes [1,7],

(i) A bound electron makes a radiative transition to another (lower) bound state of the ion (bound–bound transition: bb). The radiation power emitted during this transition is

$$P_{bb} = n(z, p)\, A(p, q)\, h\nu(p, q)\ \mathrm{J\ m^{-3}\ s^{-1}}, \qquad (1)$$

where $\nu(p, q)$ is the frequency of the emitted photon, h is Planck's constant, $n(z, p)$ is the population of the upper level of the transition and $A(p, q)$ is Einstein's spontaneous transition probability from level p to q.

(ii) An electron of the continuum makes a radiative transition to a bound level of the ion (free–bound transition: fb). Assuming Maxwellian energy distribution for the free electrons, the radiation power associated with this process is [1]

$$P_{fb} = 8.32 \times 10^{-36}\, n_e n(z, p)\, z I_{ion} \left(\frac{I_{ion}}{kT_e}\right)^{1/2}\ \mathrm{J\ m^{-3}\ s^{-1}}, \qquad (2)$$

where I_{ion} is the ionization energy from level p in eV. Dielectronic recombination may also contribute to the power associated with free–bound transitions.

(iii) An electron emits bremsstrahlung in the Coulomb field of the ions (free–free transition: ff). The radiation power associated with this process is [1]

$$P_{ff} = 4.85 \times 10^{-37}\, n_e n(z, p)\, z^2 T_e^{1/2}\ \mathrm{J\ m^{-3}\ s^{-1}}. \qquad (3)$$

The total radiative cooling rate can thus be calculated as

$$P_{tot} = P_{bb} + P_{fb} + P_{ff}. \qquad (4)$$

In the above expressions, geometrical effects and the effect of local reabsorption were neglected. It can be shown that process (ii) plays a role mainly in recombining plasmas and process (iii) at high electron temperatures (above 10 keV for the ions considered). Hence our primary aim is to determine, as accurately as possible, the power associated with bound–bound transitions, without necessitating excessive computational times. Obviously, for computing the power P_{bb}, the densities $n(z, p)$ must be known.

As is known, at low electron densities (corona limit, $n_e < 1.5 \times 10^{10}\ (kT_e)^4 \chi^{-1/2}$, both kT_e and χ are in eV, the latter being the ionization potential of the ions [8]) electron impact ionization is balanced by radiative and dielectronic recombinations, and electron impact excitation by spontaneous decay. At high electron densities ($n_e > 1.6 \times 10^{12} T_e^{1/2} \chi^3$), in the LTE limit, radiative and dielectronic recombinations are replaced by three-body recombination, and spontaneous decay by electron impact de-excitation.

Selecting a collisional–radiative model in which the rate equations for the $n(z, p)$ population densities are written in such a way, that their steady-state solution approaches the corona equilibrium values in the low electron density limit, and the LTE values in the high electron density limit, the above conditions are automatically taken into account.

In this collisional–radiative approximation, the rate

equation of the level p of ions with the charge z can be written as follows:

$$\frac{\mathrm{d}n(z,\,p)}{\mathrm{d}t} = -n(z,\,p)n_{\mathrm{e}}S(T_{\mathrm{e}},\,z,\,p) + n_{\mathrm{e}}\sum_{q\neq p}X(T_{\mathrm{e}},\,z,\,p,\,q) + \sum_{q<p}A(z,\,p,\,q) + n_{\mathrm{e}}\sum_{q\neq p}n(z,\,q)X(T_{\mathrm{e}},\,z,\,p,\,q) + \sum_{q>p}n(z,\,q)A(z,\,q,\,p) + n_{\mathrm{e}}n(z+1,\,g) \times\left\{n_{\mathrm{e}}\beta(T_{\mathrm{e}},\,z,\,p) + \alpha(T_{\mathrm{e}},\,z,\,p) + \alpha^{\mathrm{DR}}(T_{\mathrm{e}},\,z,\,p)\right\} + \delta(p-g)n_{\mathrm{e}} \times\sum_{q}n(z-1,\,q)S(T_{\mathrm{e}},\,z-1,\,q), \qquad (5)$$

where $X(T_{\mathrm{e}},\,z,\,p,\,q)$ is the electron impact excitation/de-excitation rate coefficient from level p to level q (deexcitation if q is the lower of the two levels), averaged over the Maxwellian energy distribution function, $S(T_{\mathrm{e}},\,z,\,p)$ is the electron impact ionization rate coefficient from level p, $A(z,\,p,\,q)$ is the transition probability for spontaneous decay from level p to level q, $\beta(T_{\mathrm{e}},\,z,\,p)$, $\alpha(T_{\mathrm{e}},\,z,\,p)$ and $\alpha^{\mathrm{DR}}(T_{\mathrm{e}},\,z,\,p)$ denote three-body, radiative, and di-electronic recombination rate coefficients, respectively, to level p. The step function $\delta(p-g)$ is unity if p is the ground state and is zero otherwise. This factor expresses the fact that ionization from an excited level of an ion of charge $z-1$ produces an ion in the ground state of the zth ionic charge level. In order to check whether or not dielectronic recombination (DR) plays an essential role in the processes considered, detailed check calculations were performed for carbon. The DR rates and the associated radiation power were calculated on the basis of the expressions given in [1,9]. The results showed that for electron temperatures between 10^2 and 10^3 eV radiation emission associated with DR is substantial and its relative weight increases with increasing electron density. However, in the temperature domain of our interest ($T_{\mathrm{e}} = 1$ to 10^2 eV) the contribution of dielectronic recombination to the total emissive power is negligible. For this reason, we neglected DR throughout the present analysis.

The lifetime of an excited state cannot be longer than that determined by the radiative decay rate from that particular state to lower states, whereas the lifetime of the ground state cannot be shorter than that determined by the ionization rate, which is usually the smallest among the rates influencing the ground state. Radiative lifetimes are of the order of $10^{-7}/z^4$ s for allowed (i.e. strong) transitions. Hence for time scales greater than the one given by this lifetime a quasi-steady-state solution of the rate equations can be used. As a result of this, instantaneous relaxation among the excited levels can be assumed and the time derivatives in Eq. (5) can be set to zero (except for levels with $p = g$).

Let us now add-up all equations of Eq. (5) for a given z (ionic charge number). Let $N(z)$ be the sum of all populations $n(z,\,p)$ including the ground state ($N(z) = \sum_{\mathrm{p}} n(z,\,p)$). Denoting the ionization and recombination rates from and to the level p by $S(z,\,p)$ and $R(z,\,p)$, respectively, we have for the total ion densities (including ions with different internal excited states)

$$\frac{\mathrm{d}N(z)}{\mathrm{d}t} = -\sum_{p}S(z,\,p)n(z,\,p) + \sum_{p}R(z,\,p)n(z+1,\,g) - \sum_{p}R(z-1,\,p)n(z,\,g) + \sum_{p}S(z-1,\,p)n(z-1,\,p). \qquad (6)$$

To calculate the right hand side of Eq. (6), one needs to know the populations $n(z,\,p)$.

Considering the solution of the set of Eqs. (5) and (6), there exist two alternatives.

First, the ion densities of different charge states $N(0)$, $N(1)$, …, $N(z)$ may be obtained as functions of time from independent rate computations. Once the ion densities are known, the set of equations $(\mathrm{d}n(z,\,p))/(\mathrm{d}t) = 0$ (see Eq. (5)) is solved, whereas the ion densities $N(z) = \sum_{\mathrm{p}} n(z,\,p)$ are used as normalization factors at each time level t. As a result of this procedure, the population densities of the excited levels are obtained. With the population densities known, the total radiated power can readily be calculated.

Secondly, the ion densities of different charge states $N(0)$, $N(1)$, …, $N(z)$, are given for an arbitrary initial time instant $t = 0$, and with these densities as normalization factors ($N(z) = \sum_{\mathrm{p}} n(z,\,p)$) quasi-steady-state solutions are sought for Eq. (5) $(\mathrm{d}n(z,p))/(\mathrm{d}t) = 0$. Next, with the help of the $n(z,\,p)$ populations thus found, the ion densities $N(z)$ are recalculated by means of Eq. (6). With the new $N(z)$ values known, Eq. (5) can again be solved for obtaining new $n(z,\,p) - s$ (a self-consistent iterative procedure).

This steady-state-approximation is valid for time scales larger than the time needed to establish quasi-steady-state among the excited levels. Once the $n(z,\,p)$ populations are known, the total radiated power can easily be calculated by means of (i), (ii) and (iii).

Our calculations were limited until now to the first alternative.

For the electron impact ionization rate the following expression was used [1,7,15]:

$$S(T_e, z, p) = 2.34 \times 10^{-7} \frac{\xi T_e^{1/4}}{\chi(z, p)^{7/4}} \times \exp\left(-\frac{\chi(z, p)}{kT_e}\right) \text{m}^3\ \text{s}^{-1}. \quad (7)$$

Here $\chi(z, p)$ (eV) denotes the ionization potential from level p, and ξ is the number of equivalent electrons of the level p.

The electron impact excitation rate coefficient was computed on the basis of the expression

$$X(T_e, p, q) = \frac{1.71 \times 10^{-9} g_{\text{eff}} f(p, q)}{\chi(p, q) T_e^{1/2}} \times \exp\left(-\frac{\chi(p, q)}{kT_e}\right) \text{m}^3\ \text{s}^{-1} \quad (8)$$

proposed by various authors [10–16]. Here $f(p, q)$ denotes the absorption oscillator strength, $\chi(p, q)$ is the excitation energy in eV and g_{eff} is an effective Gaunt factor [12]. It is given (tabulated) as a function of $(kT/\chi)^{1/2}$. The electron impact de-excitation rate

$$X(T_e, q, p) = \frac{g_q}{g_p} \exp\left(\frac{\chi(p, q)}{kT_e}\right) X(T_e, p, q) \quad (9)$$

was calculated in such a way as to obtain the Boltzmann distribution among the excited levels in the LTE limit. Here g_p and g_q represent the statistical weights of the levels p and q, respectively.

The radiative recombination rate coefficient was taken to be [1]

$$\alpha(T_e, z+1, p) = 2.05 \times 10^{-18} \frac{\chi(z, g)}{T_e^{1/2}}\ \text{m}^3\ \text{s}^{-1}. \quad (10)$$

The three-body recombination rate

$$\beta(T_e, z, p) = \frac{2.07 \times 10^{-22}}{LT_e^{3/2}} \exp\left(\frac{\chi(z, g)}{kT_e}\right) \times S(T_e, z, p)\ \text{m}^3\ \text{s}^{-1} \quad (11)$$

was calculated from the condition that, in the high-electron-density (LTE) limit, the populations of the successive ionization stages must correspond to the Saha equilibrium values.

The transition probabilities were taken from [17–20]. The exited levels considered are pre-selected on the basis of their radiative powers. Their number is limited to a level at which the addition of new levels increases the radiation power by less than 1%. For example, in the case of singly ionized carbon, the inclusion of only three terms from each of the transition arrays $2s^2 2p–2s2p^2$ and $2s2p^2–2p^3$ was found to be satisfactory.

3. Results and discussion

First, results obtained with the present model in the low-density limit were compared with those of Post–Jensen (PJ) [1–3]. For this purpose, an electron density of 10^{19} m^{-3} and an ion density of 10^{18} m^{-3} were assumed for both models and the emission power was computed for different temperatures. Calculations were performed for three elements: carbon, neon, and silicon. The results of comparative calculations are displayed in Fig. 1: solid lines denote results obtained with the present non-LTE model and broken lines results stemming from the PJ model. We continued the computations in the low-temperature region by recognizing the fact that the corona-equilibrium conditions are not likely satisfied in this domain.

In the case of carbon and neon, in spite of the fact that dielectronic recombination is neglected in our model, good correspondence is observed between the results of the present CR and the PJ corona equilibrium models (the deviations being not larger than those existing among the various corona-equilibrium models reviewed in [3]). In the case of Si, the deviation between the results of the two models is somewhat larger. In this case, in the low-temperature region not accessed by the PJ model, a third peak is found at around 4 eV. Although this emission is likely irrelevant under corona equilibrium conditions, it may gain relevance for non-LTE plasmas (it is due to rather intense VUV lines of the Lyman and Balmer series that sodium-like Si emits at this temperature).

After checking the convergence of the model to corona-equilibrium in the low-electron-density limit, some scenario calculations were performed. In the scenarios considered, a pellet is enclosed by a magnetic flux tube of a magnetic confinement machine (tokamak) and is heated by the incident electrons and ions of the background plasma. The heating of the pellet and of the vapor cloud (ablation products) surrounding the pellet, the ionization process and the expansion of the ablated material along the magnetic field lines are calculated by a time-dependent 1-D code in a self-consistent manner [21]. In the cases considered here, the radiation losses are calculated by means of the PJ routine. At a certain time instant, the computation is interrupted and, for the plasma parameter distributions given at that time (temperature, electron density, populations of the ion levels, etc.), the distribution of the radiation emission is recomputed also by means of the present CR model.

Fig. 2(a)–(d) correspond to a neon pellet scenario. The plasma and pellet parameters used in simulation are as follows: $T_{e0} = 0.73$ keV, $n_{e0} = 5.5 \times 10^{19}$ m^{-3}, $r_{\text{pel}} = 1$ mm, and $r_{\text{cld}} = 6.7$ mm, where r_{pel} and r_{cld} denote pellet and cloud (flux tube) radii, respectively. The distributions correspond to a time instant 15 μs after the ablation

started. The length of the expanding partially ionized carbon cloud is about 31 cm at this time. The temperature, density, and electron density distributions are shown in

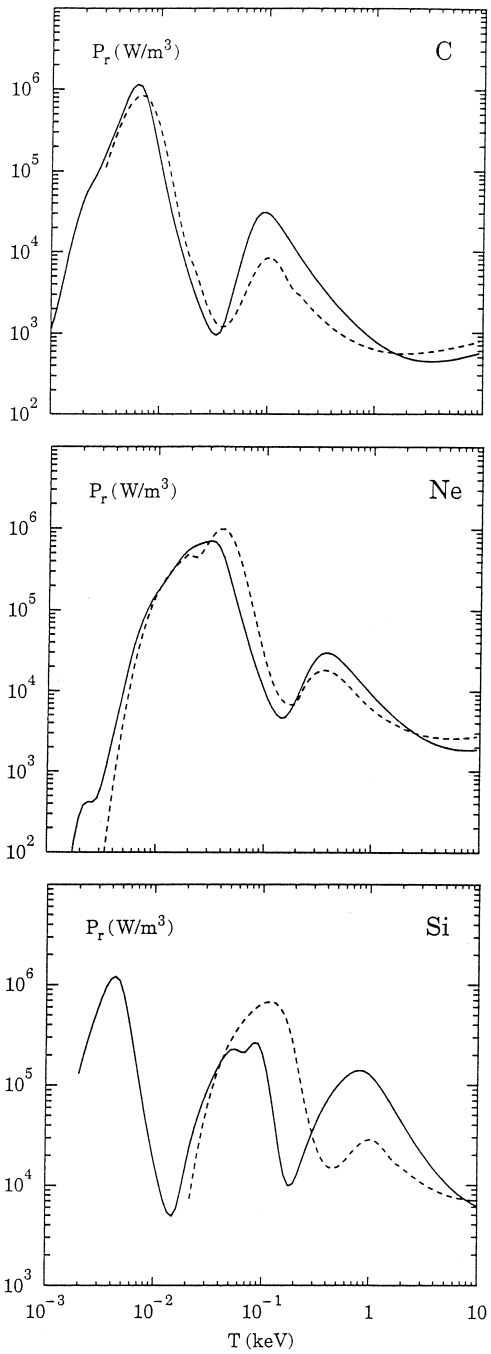

Fig. 1. Comparison of the present collisional–radiative (CR) model in the corona-equilibrium limit with the Post–Jensen model [1] for three elements: carbon, neon and silicon. Solid lines: CR model, dotted lines: PJ model.

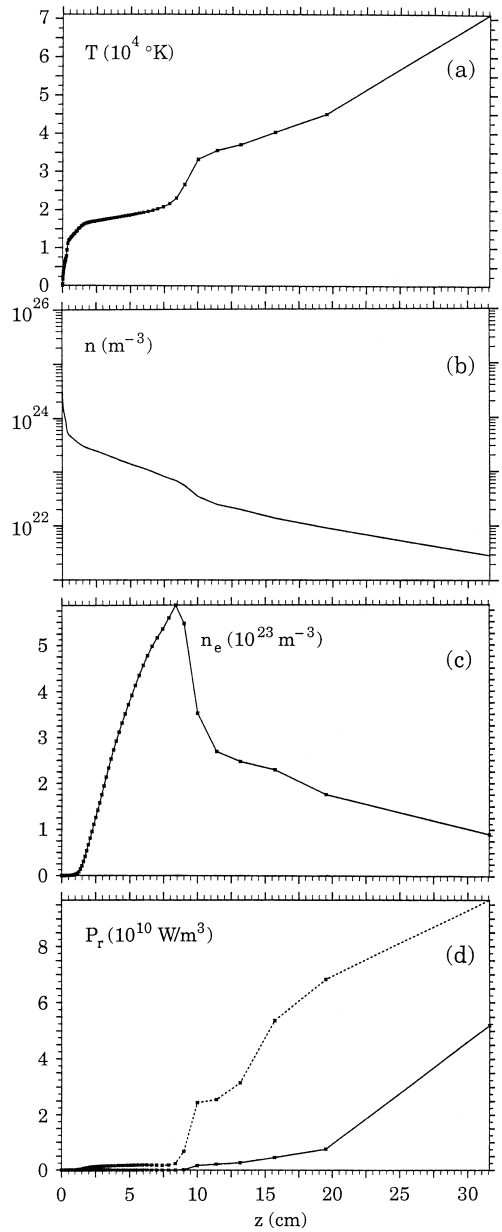

Fig. 2. The neon pellet ablation and cloud expansion scenario considered. Background (deuterium) plasma and pellet parameters: $T_{e0} = 0.73$ keV, $n_{e0} = 5.5 \times 10^{19}$ m^{-3}, $r_{cld} = 7$ mm and $r_{pel} = 1$ mm. Time = 15 μs following pellet–plasma contact. (a) Temperature distribution along the flux tube, (b) neon density ($n_a + n_i$) distribution, (c) electron density distribution. (d) Comparison of the radiated power densities computed by the CR model (dotted line) and by the PJ model (solid line) for the parameter distributions displayed.

Fig. 2(a)–(c). The distribution of the radiation power emitted per unit volume is shown in Fig. 2(d) for the two models compared (solid line = our CR approximation, bro-

ken line = PJ routine). As can be seen, in the region where notable radiation results ($z > 10$ cm), the CR model predicts approximately twice the radiation intensity given by the PJ model. The same is true for the total (time- and volume-integrated) radiation losses. In the low-temperature high-density region ($z < 7.5$ cm), the results of the two models differ by several orders of magnitude (those corresponding to the CR model being higher), but are negligible all-together. The notable increase of the radiation emission over the value predicted by the PJ model can likely be attributed to three-body recombination at the impurity densities considered (two to four orders of magnitude higher than the usual tokamak plasma densities). In corona models, three-body recombination is usually ignorable because of the inherently low electron density values.

The curves corresponding to a carbon pellet scenario are given in Fig. 3(a)–(d). Due to the much higher sublimation energy of carbon particles (compared with neon), the resulting ablation rates and cloud pressures are lower and the expansion velocities smaller. The distributions displayed in these plots correspond to 60 μs after the beginning of the ablation process. The cloud length is about 5.5 cm at this time. The plasma and pellet parameters used here are: $T_{e0} = 0.5$ keV, $n_{e0} = 6.2 \times 10^{19}$ m^{-3}, $r_{pel} = 0.63$ mm, $r_{cld} = 10$ mm. Owing to the lower background plasma temperature, the cloud temperature is low over a large fraction of the cloud length. The radiation power curves computed by the two approximations are given in Fig. 3(d). The CR model predicts in this case radiation power densities that are higher by a factor of 4 to 6 than those stemming from the PJ model over a large fraction of the carbon cloud. Again, the difference is attributed to the relevance of three-body recombination at the electron density values of our concern. The difference is reduced at the high-temperature end of the cloud where corona equilibrium conditions are approached. Substantial differences can be observed only in the low-temperature region, where the corona equilibrium approximation does not hold anyway. The integrated power loss calculated by the CR model is, at this time level, about three times as high as that predicted by the PJ model. It should be noted that, in the CR model considered, reabsorption has been neglected. Local reabsorption may reduce the net radiation power emitted and, at the same time, change the population densities of the various levels by photo-excitation and photo-ionization processes. Since accurate calculation of the reabsorption rates involves the determination of the local optical properties of the plasma such as its opacity, and must take geometrical effects into account, it is beyond the scope of the present work. In a follow-up study, this problem too shall be considered.

In summary, a collisonal–radiative model is presented for computing the radiation losses of light element enclosures in hot plasmas under non-equilibrium conditions. The computational results approach the corona equilibrium data at low electron densities. At high densities, the CR model presented yields radiation power densities notably higher than those computed in the corona equilibrium approximation.

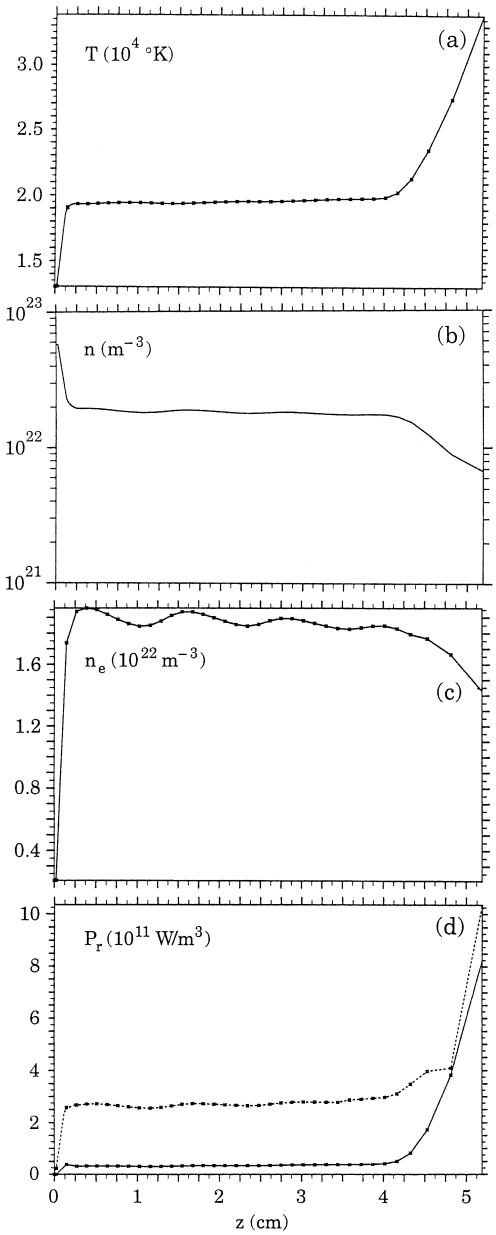

Fig. 3. The carbon pellet ablation and cloud expansion scenario considered. Background (deuterium) plasma and pellet parameters: $T_{e0} = 0.50$ keV, $n_{e0} = 6.2 \times 10^{19}$ m^{-3}, $r_{cld} = 10$ mm and $r_{pel} = 0.65$ mm. Time = 60 μs following pellet–plasma contact. (a) Temperature distribution along the flux tube, (b) carbon density ($n_a + n_i$) distribution, (c) electron density distribution. (d) Comparison of the radiated power densities computed by the CR model (dotted line) and by the PJ model (solid line) for the parameter distributions displayed.

Acknowledgements

This work was supported by the Deutsche Forschungsgemeinschaft, Project 436 UNG 13/118/2, the Hungarian Academy of Science and the National Science and Research Foundation (Grant No. F23524, 4087, and 14068). The analysis was performed during a guest-stay of the first author at Max-Planck-Institut für Plasmaphysik in Garching. The authors would like to thank D. Post for helpful discussions. Special thanks are due to K. Behringer and W. Engelhardt for critical comments. Thanks are also due to S. Kalvin and A.A. Ushakov for performing numerical checks and scenario calculations.

References

[1] D.E. Post, R.V. Jensen et al., At. Data Nucl. Data Tables 20 (1977) 397.
[2] R. Clark, J. Abdallah, D.E. Post, J. Nucl. Mater. 220–222 (1995) 1028.
[3] D.E. Post, J. Nucl. Mater. 220–222 (1995) 143.
[4] G. Pautasso, K. B'uchl et al., Nucl. Fusion 36 (1966) 1291.
[5] D.E. Post, B. Braams, N. Putvinskaya, Contrib. Plasma Phys. 36 (1996) 240.
[6] K. Behringer, private communications; H.P. Summers, At. Data and Analysis Structure Report JET-IR(94)06, 1994.
[7] R.W.P. McWhirter, Plasma Radiation in Plasma Physics and Nuclear Fusion Research, R.D. Gill (Ed.), Academic Press, New York, 1981, pp. 235–276.
[8] M.H. Key, R.J. Hutcheon, Adv. At. Molec. Phys. 16 (1980) 201.
[9] Y. Hahn, K.J. LaGattuta, Phys. Rep. 166 (1988) 1.
[10] J.C. Weisheit, J. Phys. B 8 (1975) 2556.
[11] A.K. Pradhan, J.W. Gallagher, At. Data Nucl. Data Tables 52 (1992) 227.
[12] H. Van Regemorter, Astrophys. J. 136 (1962) 906.
[13] C. Breton, D. de Michelis, M. Mattioli, J. Quant. Spectrosc. Radiat. Transfer 19 (1978) 367.
[14] R. Mewe, Astron. Astrophys. 20 (1972) 215.
[15] W. Lotz, Z. Phys. 232 (1970) 101.
[16] M.J. Seaton, Mon. Not. R. Astron. Soc. 119 (1959) 81.
[17] W.L. Wiese, M.W. Smith, B.M. Glennon, At. Transition Probabilities, H–Ne NSRDS-NBS 4, vol. 1, 1966.
[18] W.L. Wiese, M.W. Smith, B.M. Miles, At. Transition Probabilities, Na–Ca NSRDS-NBS 22, vol. 2, 1969.
[19] J.R. Fuhr, H.R. Felrice, Bibliographic database on atomic transition probabilities, at http::/physics.nist.gov/PhysRefData/fvalbib/reffrm0.html.
[20] W.L. Wiese, J.R. Fuhr, T.M. Deters, J. Phys. Chem. Ref. Data Monograph No. 7, 1996.
[21] L.L. Lengyel, P.N. Spathis, Nucl. Fusion 34 (1994) 675.